PCCP

PAPER

View Article Online
View Journal | View Issue

Cite this: *Phys. Chem. Chem. Phys.*, 2016, **18**, 9594

On the nature of bonding in binary Be_2O_2 and Si_2O_2 clusters: rhombic four-center four-electron π and σ bonds

Kang Wang,[a] Ying-Jin Wang,[a] Da-Zhi Li,*[b] Ting Ou,[a] Xiao-Yun Zhao[a] and Hua-Jin Zhai*[ac]

Received 25th January 2016,
Accepted 3rd March 2016

DOI: 10.1039/c6cp00532b

www.rsc.org/pccp

The structural and electronic properties and chemical bonding of binary Be_2O_2 and Si_2O_2 clusters have been studied using quantum chemical calculations at the B3LYP level. For the Be_2O_2 cluster, the potential energy surface is probed by unbiased structural searches and the global-minimum structure was established using the B3LYP calculations, complemented by PBE0 and single-point CCSD(T) calculations for top isomers. The perfectly planar D_{2h} Be_2O_2 (^1A_g) global minimum is well defined, being at least 3.64 eV lower in energy than alternative structures at the CCSD(T)//B3LYP/aug-cc-pVTZ level. Chemical bonding analyses show that D_{2h} Be_2O_2 and Si_2O_2 clusters possess the rhombic four-center four-electron (4c–4e) π bond, that is, the o-bond, a conception derived from electron-deficient boron oxide clusters lately. Furthermore, the Be_2O_2 and Si_2O_2 clusters also exhibit rhombic 4c–4e σ bonds, both for the radial and tangential σ frameworks (σ_r and σ_t). The σ_t framework is classified as an o-bond only formally, due to the secondary contribution from the Be/Si s component. The three-fold (π, σ_r, and σ_t) o-bonds in Be_2O_2 and Si_2O_2 are considered to resemble the three-fold aromaticity in all-metal Al_4^{2-} dianions. A 4c–4e o-bond makes use of four O 2p electrons, which would otherwise be two lone-pairs, for a delocalized and completely bonding orbital, as well as a residual nonbonding orbital. Three-fold o-bonds thus greatly stabilize the binary Be_2O_2 and Si_2O_2 clusters. We anticipate that the bonding concept should be applicable to additional molecular systems, including those with larger heterocyclic rings.

1. Introduction

During the past 20 years, tetraatomic ring-shaped clusters and relevant molecular systems have been playing a critical role in the development of new concepts for chemical bonding. Despite the simplicity in terms of structures, such small clusters offer valuable models at the molecular level, allowing a fundamental understanding of their structural and electronic properties and the nature of bonding. Notably, pentaatomic, tetracoordinate planar carbon (TPC) anions, CAl_3Si^-, CAl_3Ge^-, and CAl_4^-, were observed in the gas phase,[1–3] in which a TPC center is encircled by a tetraatomic ring. A four-center ligand–ligand σ bond is believed to be vital for stabilizing these simplest TPC clusters. Even upon removal of the TPC center, the tetraatomic ring clusters may be stable as free-standing species, as exemplified by the all-metal aromatic Al_4^{2-} cluster with 2π electrons[4] as well as the all-metal antiaromatic Al_4^{4-} cluster with 4π electrons.[5] Multiple (π and σ) aromaticity, antiaromaticity, conflicting aromaticity, and δ-aromaticity were subsequently uncovered in other main group clusters and transition metal clusters.[6–15] The nature of bonding in these novel clusters is governed by the number of valence electrons available and the manner in which the electrons occupy the specific molecular orbitals (MOs). In such bonding systems, every electron counts.

Oxide species involving main group elements are generally considered to be uninteresting in terms of chemical bonding. However, this does not seem to be true.[16–18] Recent experimental and computational studies showed, for example, that certain boron oxide clusters possess a rhombic B_2O_2 four-membered ring as the structural core, whose bonding features a four-center four-electron (4c–4e) π bond, or dubbed the o-bond.[19,20] The o-bond makes use of four O 2p electrons (due to two lone-pairs) for a completely bonding MO as well as a residual, nonbonding one. In fact, it can be traced back to the $B_2N_2H_4$ species,[21] which was first studied computationally in the 1970s and proposed to be an inorganic analogue of cyclobutadiene (C_4H_4), a prototypical

[a] *Nanocluster Laboratory, Institute of Molecular Science, Shanxi University, Taiyuan 030006, China. E-mail: hj.zhai@sxu.edu.cn*
[b] *Department of Chemical Engineering, Binzhou University, Binzhou 256603, China. E-mail: ldz005@126.com*
[c] *State Key Laboratory of Quantum Optics and Quantum Optics Devices, Shanxi University, Taiyuan 030006, China*

4π antiaromatic organic hydrocarbon. However, we showed recently *via* a theoretical study on ternary $B_2X_2H_2$ (X = O and S) clusters,[22] which are isovalent to $B_2N_2H_4$ and C_4H_4, that $B_2X_2H_2$ (X = O and S) and $B_2N_2H_4$ possess an o-bond. Such species are considered aromatic despite the 4π electron counting, differing fundamentally from the 4π antiaromaticity in C_4H_4. The concept of the rhombic o-bond[19,22] thus helps address the bonding nature of $B_2N_2H_4$ and revise a misconception of $B_2N_2H_4$ as an inorganic cyclobutadiene, which has been in existence in the literature for 40 years.

As a natural extension along this line, a couple of questions remain open: does the rhombic 4c–4e o-bond exist only for boron oxide clusters? Are there new types of o-bonds other than the π bond? Are multifold o-bonds feasible for a molecular system? The present work intends to address the above questions, using the simplest beryllium and silicon oxide clusters, Be_2O_2 and Si_2O_2, as examples. Beryllium and beryllium oxides are indispensible valuable materials in the atomic energy, missiles, rockets, and the metallurgical industry.[23] Be_2O_2 is a simple beryllium oxide cluster, but very little is presently known about the bonding nature of the alkaline-earth metal oxides.[24–26] Silicon oxide clusters provide useful model systems, which help deepen our understanding of the structures and bonding in their bulk materials.[27] Si_2O_2 is one of the silicon-rich silicon oxides and has a well-established geometric structure based on the prior studies.[27–30] It is in fact available as a synthetic compound,[30] but its nature of bonding remains to be elucidated. This study focuses on the structures and chemical bonding in Be_2O_2 and Si_2O_2 clusters.

Herein, we have performed a density-functional theory (DFT) investigation of the structural, electronic, and bonding properties of the Be_2O_2 and Si_2O_2 clusters, including computational global-minimum searches for Be_2O_2. Both Be_2O_2 and Si_2O_2 are shown to possess a rhombic D_{2h} structure. Detailed MO analyses reveal a 4c–4e π o-bond in the clusters, as well as 4c–4e σ o-bonds, which collectively render the systems multifold o-bonds. The species are considered to be aromatic rather than antiaromatic, similar in essence to the nature of bonding in the prototypical all-metal aromatic Al_4^{2-} cluster.[4] We anticipate that the current understanding should be applicable to a variety of relevant heterocyclic molecular systems.

2. Computational methods

The DFT structural searches were carried out for the Be_2O_2 cluster using the Coalescence Kick (CK) algorithm[31–33] at the hybrid B3LYP/3-21G level, aided with manual structural constructions. The CK searches have proved to be powerful in identifying the global-minimum structures for molecular systems.[33] For a small Be_2O_2 cluster, it is generally believed that the CK method is capable of exploring the potential energy surface thoroughly and thus reaching the true global minimum. A total of 499 stationary points were probed in the CK searches, many of which turned out to be duplicated structures upon reoptimizations at the higher level of theory. Subsequent structural optimizations and frequency calculations were carried out for all low-lying isomers at the B3LYP/aug-cc-pVTZ level,[34,35] where the frequency analyses were done in order to confirm that the reported structures are true minima.

For comparison and consistency, structural optimizations for the top three isomers were also performed at the PBE0/aug-cc-pVTZ level.[36] Furthermore, the relative energies for top three isomers were benchmarked using the single-point coupled-cluster CCSD(T) calculations[37–39] at the B3LYP/aug-cc-pVTZ geometry. The B3LYP and PBE0 methods produced essentially the same geometries for the isomers, with only minor differences in bond parameters. We therefore mainly focus on the B3LYP results in the following sections. Note that the B3LYP, PBE0, and CCSD(T) data are highly consistent in terms of energetics for the top isomers. The MO analyses were performed to understand the chemical bonding. The Wiberg bond indices (WBIs), natural resonance theory (NRT) bond orders, and natural atomic charges were obtained from the natural bond orbital (NBO) analyses.[40] All calculations were performed using the Gaussian 09 package.[41]

3. Results

3.1. Structural searches for the Be_2O_2 cluster

The CK structural searches for Be_2O_2 result in a number of distinct isomeric structures, whose optimized geometries at the B3LYP/aug-cc-pVTZ level are illustrated in Fig. 1, along with their bond distances and relative energies. Also shown are the relative energies at the PBE0/aug-cc-pVTZ level for the top three lowest-energy structures. The B3LYP and PBE0 data are consistent in terms of energetics for the system: 0.00, +2.88, and +3.30 eV at B3LYP *versus* 0.00, +3.24, and +3.63 eV at PBE0 (Fig. 1). As an ultimate benchmark, the single-point CCSD(T)//B3LYP/aug-cc-pVTZ calculations indicate that the relative energies for top three structures are 0.00, +3.64, and +3.69 eV, respectively, suggesting that the Be_2O_2 (**1**, D_{2h}, ^1A_g) global minimum (see Fig. 2) is rather well-defined on the potential energy surface. In the following, we will mainly discuss the B3LYP results.

While alternative isomeric structures of Be_2O_2 as shown in Fig. 1 are 3–9 eV above the Be_2O_2 (**1**, D_{2h}, ^1A_g) global minimum, we would like to comment briefly on these structures. An ideal reference structure is the fourth, trapezoid isomer: (C_{2v}, $^1A_1$, +5.96 eV). This structure can be straightforwardly described as a Be–Be unit interacting *via* two Be−O single bonds with a peroxo group O_2^{2-}, which has an O−O single bond. In other words, the Be–Be (1.95 Å), Be–O (1.46 Å), and O–O (1.53 Å) bond distances in the structure are all typical single bonds. For comparison, the Be_2 dimer as a van der Waals species has a distance of 2.45 Å,[42] whereas that of Be_2^+ is 2.21 Å (bond order: 0.5).[43] The diatomic BeO species has a distance of 1.33 Å (double bond).[44] Dioxygen (double bond) and superoxide (O_2^-; bond order: 1.5) have distances of 1.21 and 1.33 Å, respectively. Thus, in an ionic picture the trapezoid isomer is formally formulated as $Be_2^{2+}O_2^{2-}$.

The second isomer (C_s, $^1A'$) is quasi-linear, whereas the third ($C_{\infty v}$, $^1\Sigma$) is perfectly linear. These two structures differ only very slightly. The BeO group at the left side (1.35/1.33 Å) is attributed to a Be═O double bond. The OBeO fragment at the

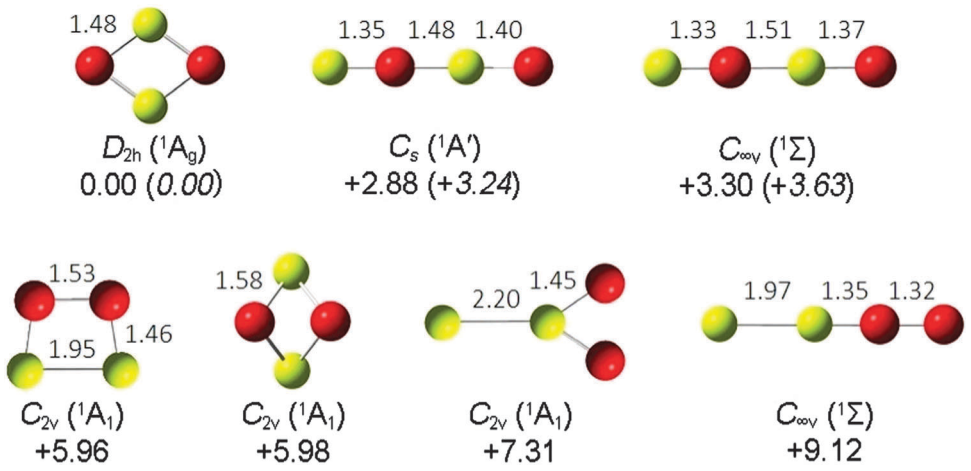

Fig. 1 Alternative optimized low-lying structures of the Be_2O_2 cluster at the B3LYP/aug-cc-pVTZ level. Relative energies are indicated in eV at B3LYP/aug-cc-pVTZ with zero point energy (ZPE) corrections, as well as at PBE0/aug-cc-pVTZ (in parentheses). Bond distances (in Å) are labeled. The Be and O atoms are in yellow and red, respectively.

right side is asymmetric (1.48/1.51 Å *versus* 1.40/1.37 Å), which probably involves a three-center four-electron (3c–4e) bond, akin to that in the OBO fragment in boron oxide clusters.[19,20] Compared to the rhombic global-minimum structure **1**, the fifth isomer has a substantial out-of-plane butterfly distortion, with a dihedral angle of 94.4° between two OBeO triangles. The Be–O distance of 1.58 Å is much longer than a single bond. On the other hand, the bond distances of O–O (1.55 Å) and Be–Be (2.03 Å) are roughly comparable to those in the trapezoid isomer. Thus the butterfly isomer may also be approximated as the interaction between the O_2^{2-} and Be_2^{2+} fragments, albeit in a three-dimensional fashion, where the Be–O bond order is 0.5 only. It may be argued that the trapezoid and butterfly isomers are interconvertible *via* a twist between O_2^{2-} and Be_2^{2+} by 90°. Interestingly, the two isomers are practically isoenergetic.

The sixth isomer is Y-shaped, in which a BeO_2 unit (with probably two Be–O single bonds) interacts with a Be atom. The Be–Be distance (2.20 Å) appears to be close to that of Be_2^+,[43] hinting the charge transfer from Be_2 to O_2 and thus there exists certain O–O interaction. Lastly, in the seventh linear isomer, ($C_{\infty v}$, $^1\Sigma$), the O–O distance of 1.32 Å is typical for superoxide, the Be–Be unit is substantially activated (1.97 Å), and there appears to be strong Be–O interaction (1.35 Å).

3.2. The D_{2h} Be_2O_2 (1) cluster as a global minimum

The global-minimum structure of Be_2O_2 (**1**, D_{2h}, ^1A_g) is depicted in Fig. 2, along with that of Si_2O_2 (**2**, D_{2h}, ^1A_g). Structure **1** is established firmly as the global minimum of Be_2O_2 *via* the CK structural searches and the B3LYP, PBE0, and single-point CCSD(T) calculations (Fig. 1), which is over 3 eV lower in energy with respect to the second low-lying isomer. It possesses a rhombic structure with a Be–O bond distance of 1.48 Å and a ∠BeOBe bond angle of 71.2° at the B3LYP/aug-cc-pVTZ level. The Be–O distance is substantially longer than that of a Be=O bond (1.33 Å),[44] yet it is comparable to a typical single bond such as that in the trapezoid isomer (1.46 Å; Fig. 1). We note that the O–O distance in **1** is 2.40 Å, which is markedly larger than that of peroxide (1.49 Å), suggesting that the direct O–O interaction in **1** is negligible, if any.

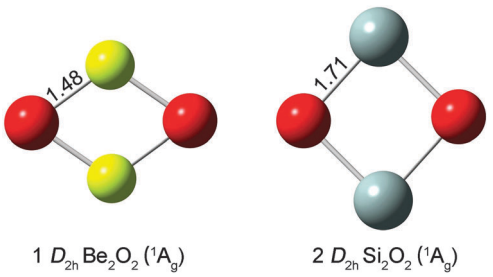

Fig. 2 Optimized global-minimum structures of D_{2h} Be_2O_2 (**1**, ^1A_g) and Si_2O_2 (**2**, ^1A_g) at the B3LYP/aug-cc-pVTZ level. Bond distances (in Å) are labeled. The bond angles ∠BeOBe and ∠SiOSi are 71.2° and 92.9°, respectively. The Be atom is in yellow, Si in gray, and O in red.

In terms of electronic properties, the calculated vertical ionization potential (IP) of **1** (D_{2h}, ^1A_g) is 10.04 eV at the B3LYP/aug-cc-pVTZ level, and the energy gap between the highest occupied and lowest unoccupied MOs (HOMO and LUMO) is 4.54 eV (see Table 1). The NBO analysis shows that the Be and O centers in **1** carry a charge of +1.28 and −1.28 |*e*|, respectively, suggesting that the Be–O bonding involves both

Table 1 Calculated Wiberg bond indices (WBIs) and natural atomic charges (*q*, in |*e*|) of the global-minimum structures of Be_2O_2 (**1**) and Si_2O_2 (**2**) at the B3LYP/aug-cc-pVTZ level. Also tabulated are the calculated HOMO–LUMO energy gaps ($\Delta E_{HOMO-LUMO}$, in eV) and vertical ionization potentials (IPs, in eV) at the same level

Species	WBI		*q*	$\Delta E_{HOMO-LUMO}$	IP
D_{2h} Be_2O_2 (**1**)	Be–O	0.61		4.54	10.04
	Be	1.31	1.28		
	O	1.27	−1.28		
D_{2h} Si_2O_2 (**2**)	Si–O	0.57		4.22	9.16
	Si	1.20	1.34		
	O	1.19	−1.34		

covalent and ionic components, as anticipated. For the previous B–O clusters,[19,20] the B and O centers have a charge of about +0.9 and −0.9 $|e|$, respectively, which are slightly more covalent. In line with the above natural charges, the calculated WBI for the Be–O bonds in **1** amounts to 0.61.

3.3. The D_{2h} Si_2O_2 (2) cluster

The planar, rhombic geometry of the Si_2O_2 cluster has been reported previously.[7–11] The optimized structure of Si_2O_2 (**2**, D_{2h}, ^1A_g) at the B3LYP/aug-cc-pVTZ level is shown in Fig. 2. It has a rhombic structure with a Si–O bond distance of 1.71 Å and a ∠SiOSi bond angle of 92.9°, suggesting that the species is quite close to a square. The O–O distance in **2** is 2.35 Å, which is similar to that in **1** (2.40 Å), indicating negligible O–O interaction in **2**. According to the latest recommended covalent radii by Pyykkö,[45,46] the upper limits for Si=O and Si–O bonds should be 1.64 and 1.79 Å, respectively. Thus, the Si–O bond in **2** is close to a single bond. The calculated WBI for Si–O is 0.57, in line with the bond distance. Note that the Si–O interaction in **2** has both covalent and ionic components (Table 1), similar to the Be–O bonding in **1**. The calculated vertical IP and HOMO–LUMO gap for **2** are 9.16 and 4.22 eV, respectively, which are both smaller than those for **1**.

4. Discussion

4.1. Four-center four-electron π bond in the rhombic D_{2h} Be_2O_2 (1) cluster

As shown in Fig. 2, both the global-minimum D_{2h} Be_2O_2 (**1**, ^1A_g) and Si_2O_2 (**2**, ^1A_g) clusters possess a rhombic X_2O_2 (X = Be and Si) four-membered heteroatomic ring. The exploration of the potential energy surface indicates that D_{2h} Be_2O_2 (**1**, ^1A_g) is well defined as the global minimum by at least ∼3 eV (Fig. 1), highlighting the robustness of the rhombic heteroatomic ring. To understand this structure, it is essential to perform a chemical bonding analysis. We choose to access the nature of bonding through the MO analysis.

The Be and O atoms have the electronic configurations of $2s^2$ and $2s^22p^4$, respectively. Since the O 2s based MOs are well below the rest of valence MOs (by 13.9 eV) at the B3LYP level, the O 2s electrons can be safely considered as lone-pairs and do not contribute to bonding in the cluster. Thus, D_{2h} Be_2O_2 (**1**, ^1A_g) has 12 valence electrons in total, whose occupied MOs are depicted in Fig. 3(a). For a ring-like system of main group elements, the s and p atomic orbitals (AOs) are capable of forming four sets of MOs: the σ_s-type (based on s AOs), p_π-type (π MOs from p AOs), σ_r-type (σ MOs based on p AOs, oriented towards the center of the ring), and σ_t-type (σ MOs based on p AOs, tangential to the ring).[6,8] These four sets are mutually uncoupled and orthogonal to each other, forming the basis of multifold electron delocalization, aromaticity, antiaromaticity, and conflicting aromaticity in the systems.

In D_{2h} Be_2O_2 (**1**, ^1A_g), the O 2s electrons are lone-pairs as described above. The Be 2s electrons interact with O in a mixed ionic/covalent manner (Table 1), undergoing substantial Be→O electron transfers. Indeed, according to the orbital composition analysis, of all MOs shown in Fig. 3(a), only HOMO−5 and HOMO−3 have a Be s component of 8% and 30%, respectively, and the Be centers participate in the majority of these MOs *via* Be p/d AOs. Thus, the bonding in **1** is dominated by Be p and O p AOs, which form the orthogonal p_π, $p_{\sigma\text{-}r}$, and $p_{\sigma\text{-}t}$ frameworks. Each framework consists of two MOs (with 4 electrons). For the π framework, HOMO−2 is the completely delocalized, complete bonding π MO, akin to that in the all-metal aromatic Al_4^{2-} cluster (HOMO; Fig. 3(b)).[4] On the other hand, the HOMO in **1** is purely nonbonding with 49% O 2p from each O center (98% in total; Table 2), complemented by 1% Be d from each Be center (2% in total). In short, HOMO−2 and the HOMO are a genuine bonding/nonbonding combination with 4π electrons, which are analogous to those in the σ-bonds for boron oxide clusters.[19,20] We can therefore conclude that D_{2h} Be_2O_2 (**1**, ^1A_g) possesses a rhombic π σ-bond.

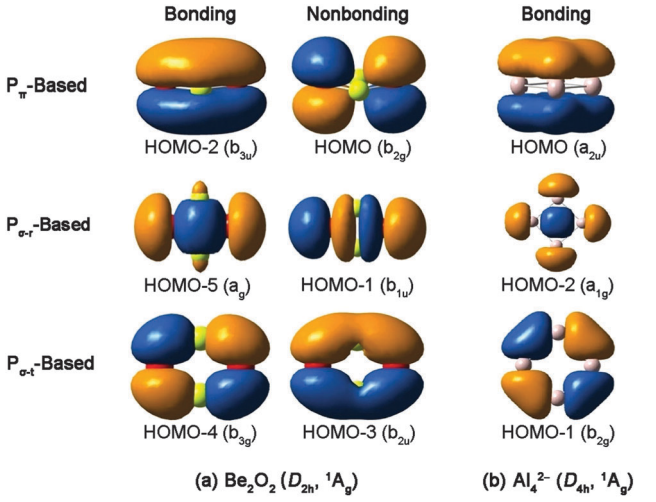

Fig. 3 Key molecular orbitals (MOs) of (a) D_{2h} Be_2O_2 (**1**, ^1A_g), as compared with those of (b) Al_4^{2-} (D_{4h}, ^1A_g). The labels p_π, $p_{\sigma\text{-}r}$, and $p_{\sigma\text{-}t}$ denote a MO derived from the np atomic orbitals (AOs) that are perpendicular to the molecular plane (π), on the molecular plane and in the radial direction (σ_r), on the molecular plane and oriented tangential to the ring (σ_t), respectively.

Table 2 Orbital composition analysis for selected nonbonding molecular orbitals (MOs) in D_{2h} Be_2O_2 (**1**, ^1A_g) and Si_2O_2 (**2**, ^1A_g), which are a critical portion of the rhombic four-center four-electron σ-bonds. Also listed are the orbital energy differences (ΔE, in eV) between the nonbonding MOs and their corresponding bonding MOs for the σ-bonds

		Orbital composition (%)				
Species	Orbital[a]	O p	O s	Be/Si	O (total)[b] (%)	ΔE
D_{2h} Be_2O_2 (**1**)	HOMO (π)	98		2 (Be d)	98	2.04
	HOMO−1 (σ_r)	82	10	6 (Be p)[c]	92	2.50
D_{2h} Si_2O_2 (**2**)	HOMO−3 (π)	96		4 (Si d)	96	2.01
	HOMO−2 (σ_r)	88	10	2 (Si d)	98	3.89

[a] Nonbonding MO as depicted in Fig. 3(a) and 4. The formal "nonbonding" σ_t MO is not included (see the text for further discussion). [b] Total contribution of the O p/s atomic orbitals to the nonbonding MO. [c] Be d component contributes the remaining 2%.

The stabilization effect of the π o-bond on **1** may be revealed by the orbital energy difference between HOMO−2 and the HOMO, which amounts to 2.04 eV (Table 2). This is a significant amount of energy considering the fact that the two MOs are primarily derived from two O 2p lone-pairs. We note that the bonding/nonbonding combination for the 4c–4e o-bond is the best way to make use of two O 2p lone-pairs for bonding in a rhombic heteroatomic ring, because it is impossible to put all four electrons into completely bonding MOs. Thus, putting the two "residual" electrons of the four in a completely nonbonding (rather than antibonding) MO, such as the HOMO, can maximize the overall bonding effect of the four electrons.

4.2. Multifold rhombic 4c–4e bonds (o-bonds) in D_{2h} Be_2O_2 (1)

As mentioned above, the p_π, $p_{\sigma\text{-}r}$, and $p_{\sigma\text{-}t}$ frameworks in rhombic D_{2h} Be_2O_2 (**1**, ^1A_g) are mutually uncoupled and orthogonal to each other.[6,8] Since the p_π framework (Fig. 3(a), top row) with a bonding/nonbonding combination of 4π electrons is firmly established to form a 4c–4e π o-bond as described in Section 4.1, it is natural to examine whether a similar bonding concept applies to the $p_{\sigma\text{-}r}$ and $p_{\sigma\text{-}t}$ frameworks as well (Fig. 3(a), middle and bottom rows). Indeed, the $p_{\sigma\text{-}r}$ and $p_{\sigma\text{-}t}$ frameworks possess $4\sigma_r$ and $4\sigma_t$ electrons, respectively, following the same electron counting as the p_π framework.

As shown in Fig. 3(a), the middle row, HOMO−5 in **1**, is the completely bonding σ_r MO between the four atoms, which is analogous to the σ_r HOMO−2 in the Al_4^{2-} cluster (Fig. 3(b)); the latter rendering σ_r aromaticity for Al_4^{2-}.[4,8] The additional σ_r MO in **1** is HOMO−1. Orbital composition analysis (Table 2) indicates that HOMO−1 contains 41% p and 5% s from each O center (92% in total for two O centers), with the minor component of 3% p and 1% d from each Be center (8% in total for two Be centers). The 92% O component for HOMO−1 suggests that the MO is essentially nonbonding in nature considering the large O–O distance in **1**. Therefore, HOMO−5 and HOMO−1 constitute a second set of bonding/nonbonding combination, which represents the σ_r framework in **1** and closely parallels the combination of HOMO−2 and the HOMO for the π framework. Following the concept of the rhombic 4c–4e π o-bond,[19,20] it is imperative to propose a rhombic 4c–4e σ o-bond for **1** on the basis of HOMO−5 and HOMO−1. It is stressed that the HOMO−5 and HOMO−1 combination also substantially stabilizes the rhombic **1** cluster, due to the sizable orbital energy difference between these MOs (2.50 eV; Table 2). If it were not for the 4c–4e σ o-bond, the four electrons are largely two O 2p lone-pairs, which would contribute negligibly to the bonding in the system.

A similar argument applies for the $p_{\sigma\text{-}t}$ framework (Fig. 3(a), bottom row), which also involves two MOs: HOMO−4 and HOMO−3. Here, HOMO−4 is again a complete bonding MO between the four atoms, due to the p AOs tangential to the ring. A similar MO, HOMO−1, renders σ_t aromaticity for the prototypical all-metal aromatic Al_4^{2-} cluster (Fig. 3(b)). For HOMO−3 in **1**, the signs of the wave function between the two O centers reverse with respect to HOMO−4, which exactly follow the changes in HOMO−2/HOMO and HOMO−5/HOMO−1. In this sense, HOMO−3 may be classified formally as "nonbonding" with respect to HOMO−4.

It should be stated that the "nonbonding" HOMO−3 is less pure as compared to the HOMO and HOMO−1, which contain 98% and 92% of O p/s components *versus* negligible 2% and 8% Be d or p components. In HOMO−3, the two O centers collectively contribute 74% p only (37% p for each O), whereas each Be contributes 15% s and −3% p. Thus HOMO−3 also contributes markedly to the σ bonding in **1**. Nonetheless, HOMO−4 and HOMO−3 in the $p_{\sigma\text{-}t}$ framework can be viewed formally as a bonding/"nonbonding" combination and approximated as a third set of 4c–4e o-bonds in **1**, that is, the rhombic 4c–4e σ_t o-bond.

In summary, the six MOs in Fig. 3(a) collectively render three-fold rhombic 4c–4e o-bonds for D_{2h} Be_2O_2 (**1**, ^1A_g). The p_π and $p_{\sigma\text{-}r}$ frameworks each possess four electrons in a relatively pure bonding/nonbonding combination, whereas the $p_{\sigma\text{-}t}$ framework exhibits only a formal bonding/"nonbonding" combination. Note that the formal "nonbonding" MO has a net bonding effect for the system, in contrast to antibonding for a typical 4-electron antiaromatic species, such as cyclobutadiene.[47,48] Overall, the bonding in **1** is contributed by four MOs, including the formal "nonbonding" HOMO−3 (but excluding the nonbonding HOMO and HOMO−1), which collectively result in a Be–O formal bond order of close to 1.0. The three-fold (p_π, $p_{\sigma\text{-}r}$, and $p_{\sigma\text{-}t}$) 4c–4e o-bonds clearly play critical roles in stabilizing the rhombic D_{2h} Be_2O_2 (**1**, ^1A_g) cluster.

4.3. Rhombic π and σ o-bonds in the D_{2h} Si_2O_2 (2) cluster

The D_{2h} Si_2O_2 (**2**, ^1A_g) cluster adopts also a planar, rhombic structure (Fig. 2), whose MOs are depicted in Fig. 4. For general

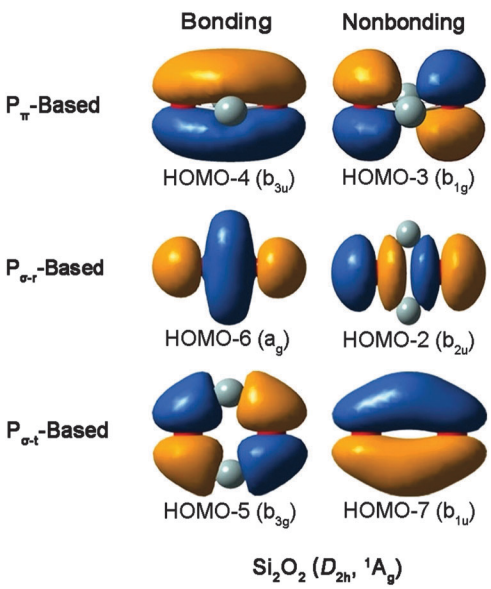

Fig. 4 Key molecular orbitals (MOs) of D_{2h} Si_2O_2 (**2**, ^1A_g). The labels p_π, $p_{\sigma\text{-}r}$, and $p_{\sigma\text{-}t}$ denote a MO derived from the np atomic orbitals (AOs) that are perpendicular to the molecular plane (π), on the molecular plane and in the radial direction (σ_r), on the molecular plane and oriented tangential to the ring (σ_t), respectively.

consideration, the Si 3s and O 2s based MOs are separated from those shown in Fig. 4 by 11.6 eV at the B3LYP level, which can be safely treated as lone-pairs. Thus, Si_2O_2 has also 12 electrons in total (Si $3p^2$ and O $2p^4$) for chemical bonding, being actually isoelectronic to the D_{2h} Be_2O_2 (**1**, ^1A_g) cluster. The calculated electronic properties of **2** and **1** do not show significant differences (Table 1). However, due to larger electronegativity of Si (1.90 at the Pauling scale) with respect to Be (1.57), the Si–O bond should be more covalent than the Be–O bond. Indeed, the electronegativity of Si is close to that of B (2.04), suggesting the viability of 4c–4e o-bonds in the D_{2h} Si_2O_2 (**2**, ^1A_g) cluster. For comparison, the electronegativity of O is 3.44.

To quantitatively describe the covalency in Be/O and Si/O bonding and compare with that in a rhombic B/O ring, we performed the NRT analyses for **1** and **2**. The Be–O bond in **1** possesses a NRT covalent bond order of 0.10 (out of a total bond order of 0.99; that is, 10%), the Si–O bond in **2** has a covalent bond order of 0.23 (out of a total of 1.03; that is, 22%), and a rhombic B/O ring in C_{2v} B_3O_3 ($^2A_1$) has a covalent B–O bond order of 0.42 out of a total of 1.46, or 29%.[19] The above trend of covalency for the Be/O, Si/O, B/O series closely correlates with the evolution of electronegativity along Be, Si, and B. The bonding covalency in Be/O and Si/O is notably revealed in the completely bonding CMOs (left column; Fig. 3 and 4).

Based on the above assessment, the D_{2h} Si_2O_2 (**2**, ^1A_g) cluster should have essentially the same bonding pattern as D_{2h} Be_2O_2 (**1**, ^1A_g). Remarkably but not surprisingly, the MOs in the p_π, $p_{\sigma\text{-}r}$, and $p_{\sigma\text{-}t}$ frameworks of **2** (Fig. 4) show one-to-one correspondence to those of **1** (Fig. 3(a)). In particular, the p_π HOMO−3 and $p_{\sigma\text{-}r}$ HOMO−2 in **2** are purely nonbonding, with the two O centers collectively contributing 96% and 98%, respectively (Table 2). The p_π HOMO−4/HOMO−3 and $p_{\sigma\text{-}r}$ HOMO−6/HOMO−2 are thus genuine bonding/nonbonding combinations, rendering rhombic 4c–4e π and σ_r o-bonds in **2**.

For the $p_{\sigma\text{-}t}$ framework, HOMO−5 is completely bonding, whereas HOMO−7 exhibits a reverse in signs of wave function for two O centers relative to HOMO−5 and is formally classified as "nonbonding". The $p_{\sigma\text{-}t}$ framework in **2** can thus be formally viewed as a rhombic 4c–4e σ_t o-bond. Again, the "nonbonding" $p_{\sigma\text{-}t}$ HOMO−7 involves secondary bonding due to the Si s component (roughly 60% O p *versus* 40% Si s), which is in contrast to the antibonding MO in a 4-electron antiaromatic species.[47,48] Based on the above discussion, the bonding in **2** is effectively due to four MOs (including HOMO−7), which lead to a Si–O bond order of around 1.0.

4.4. Simulated infrared spectra of D_{2h} Be_2O_2 (1) and Si_2O_2 (2) clusters

The infrared (IR) spectra of D_{2h} Be_2O_2 (**1**, ^1A_g) and Si_2O_2 (**2**, ^1A_g) were simulated based on the B3LYP/aug-cc-pVTZ calculations, as shown in Fig. 5. The IR spectra are similar to each other for the two species, except for a spectral shift. Two IR-active stretching modes (b_{1u} and b_{2u}) are observed in **1** at 1168 and 913 cm^{-1}, together with a weaker IR-active, out-of-plane bending mode of symmetry b_{3u} (537 cm^{-1}).

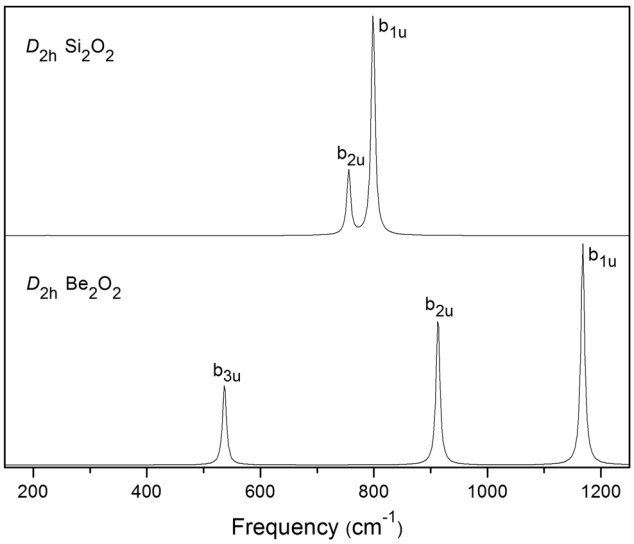

Fig. 5 Simulated infrared spectra of D_{2h} Be_2O_2 (**1**, ^1A_g) and Si_2O_2 (**2**, ^1A_g). The irreducible representations of the main vibrational modes are labeled.

For Si_2O_2 (**2**, ^1A_g), the low-frequency out-of-plane bending mode b_{3u} is negligibly weak in intensity (but not zero), situating at 225 cm^{-1}. Two other IR-active modes (b_{2u} and b_{1u}) are observed at 756 and 799 cm^{-1}, respectively, which correspond to symmetric Si–O stretchings. The b_{1u} peak is far more intense than the b_{2u} one. The IR peaks in **2** are apparently red-shifted as compared with those in **1**.

4.5. Aromaticity or antiaromaticity? Comparison of D_{2h} Be_2O_2 (1) and Si_2O_2 (2) with the all-metal aromatic D_{4h} Al_4^{2-} cluster

The multifold (p_π, $p_{\sigma\text{-}r}$, and $p_{\sigma\text{-}t}$) rhombic 4c–4e o bonds in D_{2h} Be_2O_2 (**1**, ^1A_g) and Si_2O_2 (**2**, ^1A_g) clusters suggest multifold electron delocalization in the systems. Note that each p_π, $p_{\sigma\text{-}r}$, or $p_{\sigma\text{-}t}$ framework consists of two MOs with four electrons (Fig. 3(a) and 4). A four-electron delocalized ring system has been known to be antiaromatic according to the 4n Hückel rule for antiaromaticity. So, are the **1** and **2** clusters antiaromatic? The answer is no.

As discussed above, a rhombic 4c–4e o bond in **1** or **2** represents a bonding/nonbonding combination of two MOs. Here the nonbonding MO is completely or formally nonbonding, being ascertained by two factors. First, the O components are overwhelmingly dominating the MO (by 92–98%; Table 2). Second, the O–O distances in **1** and **2** (2.35–2.40 Å) are relatively large to guarantee that there exist negligible O–O interactions, if any, in the systems. In contrast, a typical four-electron antiaromatic system possesses two MOs that are in a bonding/antibonding combination.[47,48]

For a rhombic 4c–4e o-bond, the upper MO does not have the net antibonding effect; this situation makes a 4c–4e o-bond essentially close to an aromatic 4c–2e system. Indeed, as illustrated in Fig. 3, in a 12-electron rhombic system, half of the electrons are nonbonding (at least formally). This effectively turns the system to a triply aromatic species with six-electrons (Fig. 3(b)), because the nonbonding MOs play a negligible role

in terms of aromaticity (in particular they do not have a net antibonding effect)[47,48] and should simply be neglected in counting. In short, the **1** and **2** species are considered to be aromatic rather than antiaromatic.

The nuclear independent chemical shift (NICS) is a popular computational measure of aromaticity. We calculated the NICS(1) at 1 Å above the center of the rhombus in **1** and **2**. The calculated NICS(1) values are −1.19 ppm for **1** and −0.10 ppm for **2**. While these are relatively small NICS(1) values, they are both negative, consistent with aromaticity for the species. We would like to comment that heterocyclic systems such as **1** and **2** are not anticipated to possess a highly negative NICS, because the completely bonding MOs in **1** and **2** originate primarily from the O 2p lone-pairs (Fig. 3(a) and 4), for which the delocalization is poor with respect to aromatic hydrocarbons. Indeed, the prototypical "inorganic benzene" species, $B_3O_3H_3$ (boroxine) and $B_3O_3(BO)_3$ (boronyl boroxine),[49] have NICS values of merely −3.4 and −2.8 ppm, respectively, at the B3LYP level, which is in contrast to −29.7 ppm for benzene.

5. Conclusions

In conclusion, we have explored the potential energy surface of the Be_2O_2 cluster *via* computational structural searches, and theoretically investigated the nature of bonding in rhombic D_{2h} Be_2O_2 (**1**, ^1A_g) and Si_2O_2 (**2**, ^1A_g). Both clusters can be viewed as a 12-electron system, which consists of three mutually uncoupled frameworks (π, radial σ, and tangential σ). Each framework has four-electrons in a bonding/nonbonding combination, rendering three-fold rhombic four-center four-electron o-bonds in **1** and **2**. In contrast to typical four-electron antiaromatic ring systems, the **1** and **2** species are considered to be aromatic, whose bonding essence is analogous to that of the all-metal aromatic Al_4^{2-} cluster. The present bond concept may be applicable to other main group cyclic clusters and molecules.

Acknowledgements

This work was supported by the National Natural Science Foundation of China (21573138), the State Key Laboratory of Quantum Optics and Quantum Optics Devices (KF201402), and the Natural Science Foundation of Shandong Province (ZR2014BL011).

References

1 X. Li, L. S. Wang, A. I. Boldyrev and J. Simons, *J. Am. Chem. Soc.*, 1999, **121**, 6033.
2 L. S. Wang, A. I. Boldyrev, X. Li and J. Simons, *J. Am. Chem. Soc.*, 2000, **122**, 7681.
3 A. I. Boldyrev and L. S. Wang, *J. Phys. Chem. A*, 2001, **105**, 10759.
4 X. Li, A. E. Kuznetsov, H. F. Zhang, A. I. Boldyrev and L. S. Wang, *Science*, 2001, **291**, 859.
5 A. E. Kuznetsov, K. A. Birch, A. I. Boldyrev, X. Li, H. J. Zhai and L. S. Wang, *Science*, 2003, **300**, 622.
6 H. J. Zhai, A. E. Kuznetsov, A. I. Boldyrev and L. S. Wang, *ChemPhysChem*, 2004, **5**, 1885.
7 A. I. Boldyrev and L. S. Wang, *Chem. Rev.*, 2005, **105**, 3716.
8 J. M. Mercero, A. I. Boldyrev, G. Merino and J. M. Ugalde, *Chem. Soc. Rev.*, 2015, **44**, 6519.
9 H. J. Zhai, B. B. Averkiev, D. Y. Zubarev, L. S. Wang and A. I. Boldyrev, *Angew. Chem., Int. Ed.*, 2007, **46**, 4277.
10 J. E. Fowler and J. M. Ugalde, *J. Phys. Chem. A*, 2000, **104**, 397.
11 J. I. Aihara, H. Kanno and T. Ishida, *J. Am. Chem. Soc.*, 2005, **127**, 13324.
12 H. J. Zhai, A. N. Alexandrova, K. A. Birch, A. I. Boldyrev and L. S. Wang, *Angew. Chem., Int. Ed.*, 2003, **42**, 6004.
13 H. J. Zhai, B. Kiran, J. Li and L. S. Wang, *Nat. Mater.*, 2003, **2**, 827.
14 W. Huang, A. P. Sergeeva, H. J. Zhai, B. B. Averkiev, L. S. Wang and A. I. Boldyrev, *Nat. Chem.*, 2010, **2**, 202.
15 H. J. Zhai, Y. F. Zhao, W. L. Li, Q. Chen, H. Bai, H. S. Hu, Z. A. Piazza, W. J. Tian, H. G. Lu, Y. B. Wu, Y. W. Mu, G. F. Wei, Z. P. Liu, J. Li, S. D. Li and L. S. Wang, *Nat. Chem.*, 2014, **6**, 727.
16 H. J. Zhai, Q. Chen, H. Bai, S. D. Li and L. S. Wang, *Acc. Chem. Res.*, 2014, **47**, 2435.
17 H. J. Zhai, S. D. Li and L. S. Wang, *J. Am. Chem. Soc.*, 2007, **129**, 9254.
18 S. D. Li, H. J. Zhai and L. S. Wang, *J. Am. Chem. Soc.*, 2008, **130**, 2573.
19 Q. Chen, H. G. Lu, H. J. Zhai and S. D. Li, *Phys. Chem. Chem. Phys.*, 2014, **16**, 7274.
20 W. J. Tian, L. J. Zhao, Q. Chen, T. Ou, H. G. Xu, W. J. Zheng, H. J. Zhai and S. D. Li, *J. Chem. Phys.*, 2015, **142**, 134305.
21 (*a*) N. C. Baird and R. K. Datta, *Inorg. Chem.*, 1972, **11**, 17; (*b*) N. C. Baird, *Inorg. Chem.*, 1973, **12**, 473.
22 D. Z. Li, L. J. Zhang, T. Ou, H. X. Zhang, L. Pei, H. J. Zhai and S. D. Li, *Phys. Chem. Chem. Phys.*, 2015, **17**, 16798.
23 L. Ren, L. J. Cheng, Y. Feng and X. M. Wang, *J. Chem. Phys.*, 2012, **137**, 014309.
24 C. A. Thompson and L. Andrews, *J. Chem. Phys.*, 1994, **100**, 8689.
25 T. Kobayashi, K. Seki and T. Takayanagi, *Chem. Phys. Lett.*, 2010, **498**, 235.
26 T. Kobayashi, Y. Kohno, T. Takayanagi, K. Seki and K. Ueda, *Comput. Theor. Chem.*, 2012, **991**, 48.
27 L. S. Wang, S. R. Desai, H. Wu and J. B. Nichloas, *Z. Phys. D*, 1997, **40**, 36.
28 J. S. Anderson, J. S. Ogden and M. J. Ricks, *Chem. Commun.*, 1968, 1585.
29 J. S. Anderson and J. S. Ogden, *J. Chem. Phys.*, 1969, **51**, 4189.
30 S. S. Sen, G. Tavcar, H. W. Roesky, D. Kratzert, J. Hey and D. Stalke, *Organometallics*, 2010, **29**, 2343.
31 A. P. Sergeeva, B. B. Averkiev, H. J. Zhai, A. I. Boldyrev and L. S. Wang, *J. Chem. Phys.*, 2011, **134**, 224304.
32 M. Saunders, *J. Comput. Chem.*, 2004, **25**, 621.

33 P. P. Bera, K. W. Sattelmeyer, M. Saunders and P. v. R. Schleyer, *J. Phys. Chem. A*, 2006, **110**, 4287.
34 R. A. Kendall, T. H. Dunning, Jr. and R. J. Harrison, *J. Chem. Phys.*, 1992, **96**, 6796.
35 A. D. Becke, *J. Chem. Phys.*, 1993, **98**, 5648.
36 C. Adamo and V. Barone, *J. Chem. Phys.*, 1999, **110**, 6158.
37 R. J. Bartlett and M. Musial, *Rev. Mod. Phys.*, 2007, **79**, 291.
38 J. Cizek, *Adv. Chem. Phys.*, 1969, **14**, 35.
39 G. E. Scuseria and H. F. Schaefer III, *J. Chem. Phys.*, 1989, **90**, 3700.
40 E. D. Glendening, J. K. Badenhoop, A. E. Reed, J. E. Carpenter, J. A. Bohmann, C. M. Morales and F. Weinhold, *NBO 5.0*, Theoretical Chemistry Institute, University of Wisconsin, Madison, 2001.
41 M. J. Frisch, G. W. Trucks, H. B. Schlegel, G. E. Scuseria, M. A. Robb, J. R. Cheeseman, G. Scalmani, V. Barone, B. Mennucci, G. A. Petersson, H. Nakatsuji, M. Caricato, X. Li, H. P. Hratchian, A. F. Izmaylov, J. Bloino, G. Zheng, J. L. Sonnenberg, M. Hada, M. Ehara, K. Toyota, R. Fukuda, J. Hasegawa, M. Ishida, T. Nakajima, Y. Honda, O. Kitao, H. Nakai, T. Vreven, J. A. Montgomery, Jr., J. E. Peralta, F. Ogliaro, M. Bearpark, J. J. Heyd, E. Brothers, K. N. Kudin, V. N. Staroverov, R. Kobayashi, J. Normand, K. Raghavachari, A. Rendell, J. C. Burant, S. S. Iyengar, J. Tomasi, M. Cossi, N. Rega, J. M. Millam, M. Klene, J. E. Knox, J. B. Cross, V. Bakken, C. Adamo, J. Jaramillo, R. Gomperts, R. E. Stratmann, O. Yazyev, A. J. Austin, R. Cammi, C. Pomelli, J. W. Ochterski, R. L. Martin, K. Morokuma, V. G. Zakrzewski, G. A. Voth, P. Salvador, J. J. Dannenberg, S. Dapprich, A. D. Daniels, Ö. Farkas, J. B. Foresman, J. V. Ortiz, J. Cioslowski and D. J. Fox, *GAUSSIAN 09, Revision D.01*, Gaussian, Inc., Wallingford, CT, 2009.
42 J. M. Merritt, V. E. Bondybey and M. C. Heaven, *Science*, 2009, **324**, 1548.
43 I. O. Antonov, B. J. Barker, V. E. Bondybey and M. C. Heaven, *J. Chem. Phys.*, 2010, **133**, 074309.
44 H. F. Schaefer III, *J. Chem. Phys.*, 1971, **55**, 176.
45 P. Pyykkö and M. Atsumi, *Chem. – Eur. J.*, 2009, **15**, 12770.
46 P. Pyykkö, *J. Phys. Chem. A*, 2015, **119**, 2326.
47 R. Breslow, R. Grubbs and S. I. Murahashi, *J. Am. Chem. Soc.*, 1970, **92**, 4139.
48 R. Breslow, *Acc. Chem. Res.*, 1973, **6**, 393.
49 D. Z. Li, H. Bai, Q. Chen, H. G. Lu, H. J. Zhai and S. D. Li, *J. Chem. Phys.*, 2013, **138**, 244304.